Noncoding RNAs of Trithorax Response Elements Recruit *Drosophila* Ash1 to Ultrabithorax

Tilman Sanchez-Elsner,[1] Dawei Gou,[1] Elisabeth Kremmer,[2] Frank Sauer[1]*

Homeotic genes contain cis-regulatory trithorax response elements (TREs) that are targeted by epigenetic activators and transcribed in a tissue-specific manner. We show that the transcripts of three TREs located in the *Drosophila* homeotic gene *Ultrabithorax* (*Ubx*) mediate transcription activation by recruiting the epigenetic regulator Ash1 to the template TREs. TRE transcription coincides with *Ubx* transcription and recruitment of Ash1 to TREs in *Drosophila*. The SET domain of Ash1 binds all three TRE transcripts, with each TRE transcript hybridizing with and recruiting Ash1 only to the corresponding TRE in chromatin. Transgenic transcription of TRE transcripts restores recruitment of Ash1 to *Ubx* TREs and restores *Ubx* expression in *Drosophila* cells and tissues that lack endogenous TRE transcripts. Small interfering RNA–induced degradation of TRE transcripts attenuates Ash1 recruitment to TREs and *Ubx* expression, which suggests that noncoding TRE transcripts play an important role in epigenetic activation of gene expression.

The identity of cells in metazoan organisms is established during development and mitotically propagated throughout the entire life cycle. Phylogenetically highly conserved protein families of epigenetic regulators determine the fate of developing cells by establishing and maintaining mitotically stable gene expression programs (*1*–*4*). In *Drosophila*, members of the trithorax group (trxG) of epigenetic regulators maintain active transcription states, whereas members of the Polycomb group (PcG) maintain repressed transcription states (*2*–*4*). Many epigenetic regulators control gene expression by establishing transcriptional competent or silent chromatin structures (*5*, *6*). Several epigenetic activators [Trx, trithorax-related (Trr)] and repressors (Enhancer of zeste) are lysine-specific histone methyltransferases (HMTs) and contain a SET domain, the catalytic hallmark motif of HMTs. Methylation of lysine residues in histones H3 and H4 has been correlated with epigenetic activation [Lys^4 in H3 (H3-K4)] and repression [Lys^9 and Lys^{27} in H3 (H3-K9)] (*6*–*8*).

We previously showed that the epigenetic activator "absent small and homeotic discs" (Ash1) promotes transcriptional activation by trimethylating H3-K4, H3-K9, and Lys^{20} in H4 (H4-K20) (*9*). Ash1 maintains activated transcription states in larval imaginal discs that give rise to the appendages in the adult fly (*10*, *11*). For example, Ash1 is essential for the expression of the homeotic gene *Ultrabithorax* (*Ubx*) in third-leg and haltere imaginal discs, and *Ubx* expression coincides with Ash1-mediated histone methylation (*9*–*11*).

PcG and trxG regulators are recruited to specific chromosomal elements that are present in the cis-regulatory region of target genes (*2*–*4*). The same element can act as an activating or a silencing module (*4*). In the repressed state, the elements represent Polycomb response elements (PREs) and facilitate the recruitment of PcG proteins (*2*–*4*). In the activated state, the DNA-elements function as trithorax response elements (TREs) and recruit trxG proteins (*3*, *4*). Transcription of noncoding RNAs (ncRNAs) from TRE/PRE elements switches silent PREs into TREs, which indicates that TRE/PRE transcription plays an important role in epigenetic activation (*12*–*15*). How transcription of TREs culminates in the recruitment of trxG regulators is unknown. Here, we address the question of how epigenetic regulators without known DNA binding capabilities, such as Ash1 (*16*), recognize and bind target genes in chromatin.

***Ubx* TREs are transcribed in *Drosophila* imaginal discs.** The coincidence of the tissue-specific transcription and trans-regulatory activity patterns of TREs and trxG proteins, respectively, suggests that not only TRE/PRE transcription but also the resulting ncRNAs might play a role in epigenetic activation (*12*–*15*). Here, we analyze the role of ncRNAs transcribed from three *Ubx* TRE/PREs. The *Ubx* locus contains a cluster of three characterized TRE/PREs (TRE1 to TRE3) within the boundaries of the chromosomal memory element (CME) *bxd* that is located 22 kb upstream of the *Ubx* promoter (Fig. 1A) (*17*, *18*).

To correlate the transcriptional activity of *Ubx* with *bxd* transcription in *Drosophila*, we used rapid amplification of cDNA ends (RACE) to detect *bxd* transcripts in third-leg discs. Three capped, polyadenylated *bxd* transcripts transcribed by RNA polymerase II were detected in third-leg and haltere discs (*tre1*, *tre2*, *tre3*) (Fig. 1A) (*19*).

We next used the reverse transcription polymerase chain reaction (RT-PCR) to determine

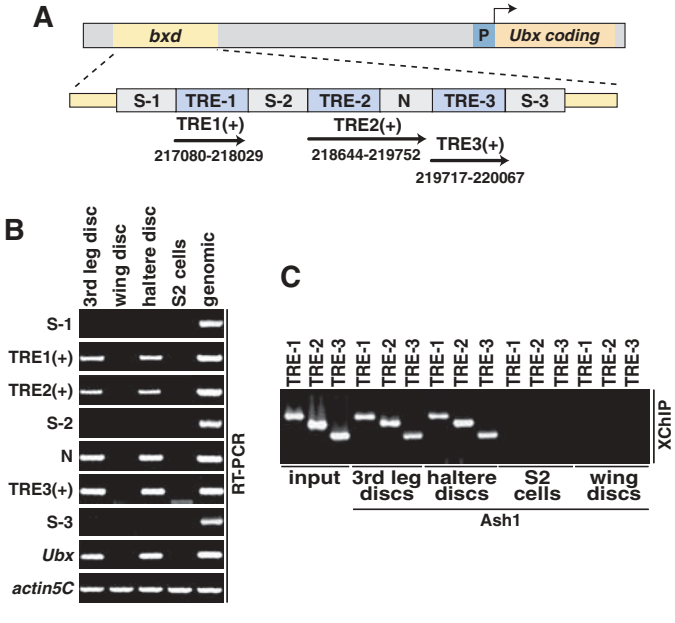

Fig. 1. Cell type–specific transcription of *Ubx* TREs. (**A**) Schematic representation of the *Ubx* locus (top) and the *bxd* DNA element (bottom). The positions of *bxd*, *Ubx* promoter (P), TREs, spacer DNA (S-1, S-2, N, and S-3) are indicated. The orientation and position (*22*) of TRE transcripts in *bxd* are indicated. (**B**) RT-PCR assays were used to detect the transcripts of the indicated *bxd* elements and control transcripts (*actin5C*, *Ubx*) in imaginal discs (third-leg, haltere, and wing), Schneider S2 cells, and genomic DNA. (**C**) PCR analysis of XChIP immunoprecipitates detecting the association of Ash1 with *Ubx* TREs in imaginal discs and S2 cells. Input represents the amount of transcripts or TREs detected in 0.5% of the starting material.

[1]Department of Biochemistry, University of California, Riverside, CA 92521, USA. [2]Institut für Molekulare Immunologie, GSF-Forschungszentrum für Umwelt und Gesundheit, Marchioninistr. 25, 81377 München, Germany.

*To whom correspondence should be addressed: E-mail: frank.sauer@ucr.edu

whether the presence of the three TRE transcripts coincides with *Ubx* transcription. RNA was isolated from third-leg discs and haltere imaginal discs (haltere discs), which both transcribe *Ubx*, and from wing imaginal discs (wing discs) and embryonic *Drosophila* Schneider 2 (S2) cells that do not transcribe *Ubx* (*9*–*11*). Transcripts from *Ubx* and all three TREs were detected in third-leg and haltere discs, whereas *Ubx* and TRE transcripts were not detected in S2 cells and wing discs (Fig. 1B) (figs. S1 and S2).

Recruitment of Ash1 to *Ubx* TREs. To investigate whether Ash1 is recruited to transcriptionally active *Ubx* TREs, we used in vivo cross-linked chromatin immunoprecipitation (XChIP) to detect Ash1 at the *Ubx* TREs in third-leg, haltere, and wing discs and in S2 cells, all of which express *ash1* (*9*, *10*). Ash1 was detected at all three TREs in third-leg and haltere discs (Fig. 1C). In addition, the characteristic Ash1 histone methylation pattern was detectable in all three TREs and the transcriptionally active *Ubx* promoter in third-leg discs (Fig. 1C and Fig. 2A). Ash1 was not detected at the TREs of the transcriptionally inactive *Ubx* locus in wing discs and S2 cells, which do not transcribe TREs (Fig. 1C).

We also compared the recruitment of Ash1 to *Ubx* in wild-type and homozygous mutant $ash1^{22}$ third-leg discs by XChIP. The $ash1^{22}$ mutant is recessive lethal and expresses a truncated protein that lacks the SET domain and trans-activation activity (*10*). Ash1 and the characteristic Ash1 histone methylation pattern were detected at the transcriptionally active *Ubx* locus in wild-type discs but not in $ash1^{22}$ mutant discs (Fig. 2, A and B) (fig. S3); this finding indicates that recruitment of Ash1 and Ash1-mediated histone methylation coincides with activation of *Ubx* expression in third-leg discs. We monitored TRE transcription in the wild-type and $ash1^{22}$ mutant third-leg discs by RT-PCR. TRE transcripts were detected at comparable levels in wild-type and mutant discs, which indicates that Ash1 is not a major regulator of TRE transcription in imaginal discs (Fig. 2C) (fig. S3).

Ash1 SET domain interacts with TRE transcripts in vitro. The association of Ash1 with TREs in cells producing TRE transcripts suggests that TRE transcription or TRE transcripts nucleate recruitment of Ash1 to *Ubx* TREs. SET-domain proteins can bind single-stranded RNA and DNA in vitro, and ncRNA has been implicated in protein recruitment in gene dosage compensation (*20*–*24*). We used in vitro protein-RNA binding assays to assess whether Ash1 associates with TRE transcripts. Ash1SET, which consists of amino acids 1001 to 1619, retained TRE1(+), TRE2(+), and TRE3(+) but not the H3-K9–specific HMT Medusa (Mdu) (Fig. 3A) (fig. S4). In contrast, Ash1, Ash1ΔN, and Mdu did not bind the antisense RNA of the *Ubx* TREs (Fig. 3A) (fig. S4). Ash1ΔN did not interact with the N-element in *tre2* (Fig. 3A), which corresponds to the DNA spacer separating TRE-2 and TRE-3 (Fig. 1A).

In competition experiments, unlabeled TRE transcripts could outcompete the interaction of Ash1 with the corresponding TRE transcript (fig. S5). In contrast, double-stranded TRE transcripts, double-stranded DNA TRE sequences, and DNA-RNA hybrids consisting of TRE transcripts and TREs failed to disrupt the interaction; these findings suggest that Ash1 associates with single-stranded TRE transcripts (fig. S5).

To delineate the RNA-binding motif of Ash1, we investigated the interaction of truncated *ash1* proteins with TRE transcripts. In addition to Ash1SET, we tested Ash1ΔN (amino acids 1001 to 2218), which contains the Ash1 SET module, and Ash1N (amino acids 1 to 1001) and Ash1C (amino acids 1619 to 2218), which both lack the SET domain and cysteine-rich regions (Fig. 3B). Ash1ΔN and Ash1SET, but not Ash1N and Ash1C, retained TRE transcripts, indicating that the SET domain of Ash1 binds TRE transcripts in vitro (Fig. 3C).

RNA-dependent recruitment of Ash1 to *Ubx* TREs in *Drosophila*. We next used XChIP to investigate whether Ash1 associates with TRE transcripts in vivo. Ash1 coprecipitated with TRE transcripts but not control transcripts from mock-treated chromatin (Fig. 3D) (fig. S6). Ash1 bound TRE transcripts in ribonuclease (RNase) III–treated chromatin, indicating that double-stranded RNA (dsRNA) motifs within TRE transcripts do not mediate the association of TRE transcripts with Ash1 in vivo (Fig. 3D) (fig. S7). In contrast, Ash1 did not interact with TRE transcripts from RNase A– and RNase H–treated chromatin, indicating that single-stranded RNA (ssRNA) is important for the association of Ash1 with TRE transcripts (Fig. 3D) (fig. S7). The disruption of the association between Ash1 and TRE transcripts by RNase H (which degrades DNA-RNA hybrids) in chromatin suggests that TRE transcripts hybridize with DNA in chromatin.

Is the association of Ash1 with TREs dependent on RNA? We used XChIP to compare the interaction of Ash1 and TRE in mock- and RNase-treated chromatin. Antibodies to Ash1 precipitated all three TREs, but not the spacer DNAs (S-2), from mock-treated and RNase III–treated chromatin, indicating that dsRNA does not contribute to the interaction of Ash1 with TREs (Fig. 3E) (fig. S7). In contrast, treating chromatin with RNase H or RNase A attenuated the association of Ash1 with TREs, indicating that the association of Ash1 with the *Ubx* TREs is RNA-dependent (Fig. 3E) (fig. S7). The disruption of the interaction of Ash1 with TREs in chromatin by RNase H and RNase A raises the possibility that ssRNA motifs in RNA-DNA hybrids play a role in the recruitment of Ash1 to TREs.

To verify that the observed attenuation of Ash1-TRE interactions is based on specific rather than general disruption of protein-DNA interactions in RNase-treated chromatin, we investigated the recruitment of the general transcription factor TFIID to target genes in mock- and RNase-treated chromatin (*25*). The TATA-binding protein (TBP) subunit of TFIID

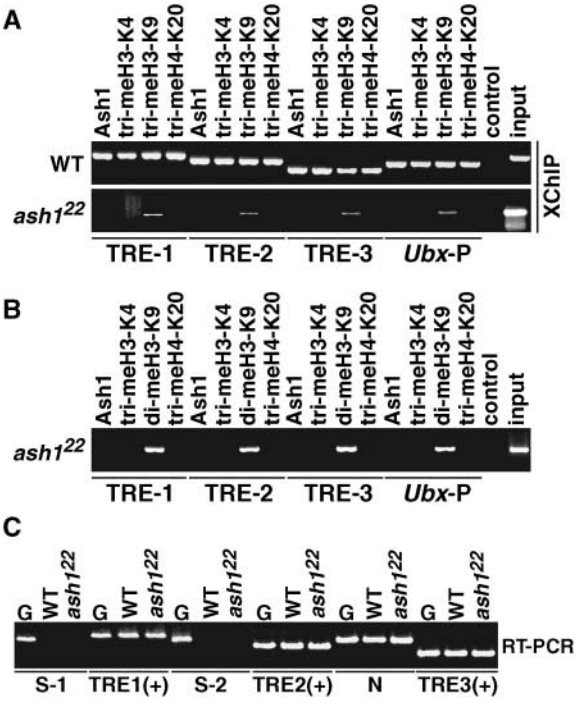

Fig. 2. Recruitment of Ash1 to *Ubx* TREs in third-leg imaginal discs. (**A**) PCR analysis of XChIP immunoprecipitates detecting the association of Ash1 and the Ash1 histone methylation pattern at the TREs and promoter of *Ubx* in wild-type (WT) and $ash1^{22}$ mutant third-leg imaginal discs. In vivo cross-linked chromatin was immunoprecipitated with the indicated antibodies and rat/rabbit antiserum (control). Input represents the amount of TRE-1 detected in 0.5% of the starting material. (**B**) XChIP analysis as described in (A), except that chromatin was immunoprecipitated with an antibody to di-methylated H3-K9. (**C**) RT-PCR analysis detecting *bxd* transcripts in RNA pools isolated from wild-type (WT) and $ash1^{22}$ mutant third-leg discs or in genomic DNA (G).

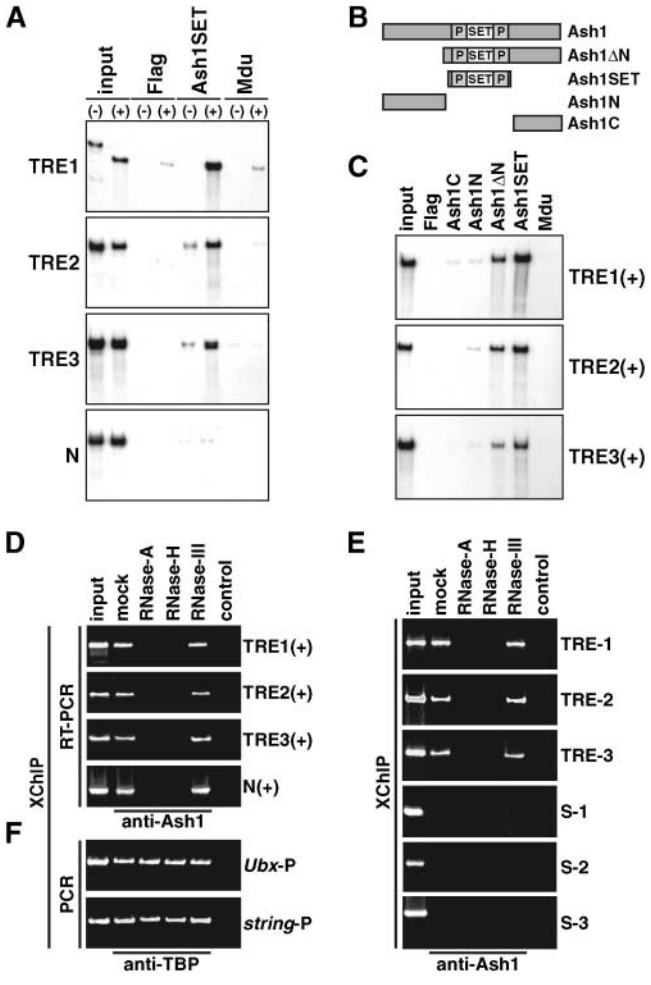

Fig. 3. The SET domain of Ash1 binds TRE transcripts in vitro and in chromatin. (**A**) Autoradiograms of in vitro protein-RNA binding assays (*19*). Radiolabeled sense (+) and antisense (–) transcripts of TRE-1, TRE-2, N, and TRE-3 were incubated with anti-Flag M2 antibody agarose (Flag) or Flag beads loaded with recombinant Ash1SET or Medusa (Mdu). (**B**) Schematic representation of Ash1 and truncated Ash1 derivatives. The position of the SET domain (SET) and pre- and post-SET domains (P) are indicated. (**C**) In vitro protein-RNA binding assays as in (A), except that Flag beads were loaded with Ash1SET, Ash1ΔN, Ash1C, or Ash1N (amino acids 1 to 1001). In (A) and (C), input represents 10% of the input RNA. (**D**) PCR analysis of XChIP immunoprecipitates detecting the association of Ash1 with *bxd* transcripts in mock and RNase-treated and subsequently cross-linked chromatin isolated from third-leg discs. (**E**) XChIP assays were used to detect the association of Ash1 with TREs in chromatin. (**F**) XChIP assays were used to detect the association of TBP to the *Ubx* promoter (*Ubx*-P) and *string/cdc25* promoter (*string*-P) in precipitated DNA pools. In (D) to (F), input represents DNA and RNA detected in 0.5% of the input material.

interacts with the TATA box in eukaryotic promoters (*25*). PCR detected the interaction of TBP with the promoter of *Ubx* and *string*, whose transcription requires TFIID activity (*26*). TBP interacted with both promoters in mock-treated and RNase A–, RNase H–, and RNase III–treated chromatin, indicating that RNase treatment did not attenuate TBP-promoter interactions and protein-gene interactions in general (Fig. 3F) (fig. S7).

To test whether the detected association of Ash1 with TREs and TRE transcripts occurs in chromatin or is the result of fortuitous interactions generated in chemically cross-linked chromatin, we investigated the association of Ash1 with TRE transcripts and TREs in native chromatin with the use of native chromatin immunoprecipitation (NChIP). Ash1 bound all three TREs and TRE transcripts in mock- and RNase III–treated chromatin but not in RNase H– or RNase A–treated chromatin, indicating that Ash1 coimmunoprecipitates with TREs and TRE transcripts in native chromatin (Fig. 4, A and B) (fig. S8). An association of Ash1 with the N portion of the TRE2(+) transcript, as observed in cross-linked chromatin, was not detectable in native chromatin; this result indicates that, as in vitro, Ash1 binds the RNA corresponding to TRE-2 but not the N region of the TRE2(+) transcript.

Collectively, our data indicate that the recruitment of Ash1 to the TREs of *Ubx* is mediated by RNA and suggests the existence of a trimeric protein–nucleic acid complex in chromatin, consisting of Ash1, TREs, and TRE transcripts.

Ash1 is detectable at about 150 loci on *Drosophila* polytene chromosomes (*10*). To assess whether RNA facilitates Ash1 recruitment to target loci other than *Ubx*, we compared the interaction of Ash1 with target loci on

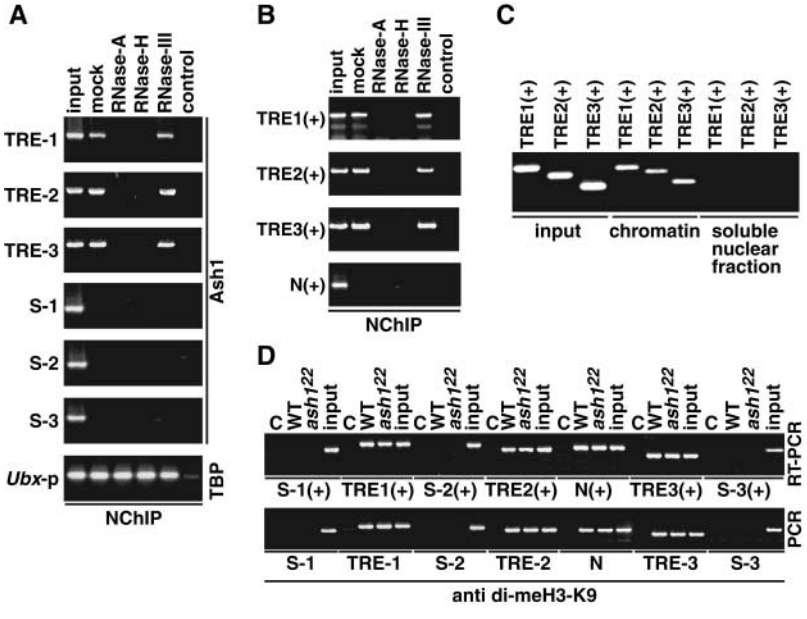

Fig. 4. TRE transcripts mediate the recruitment of Ash1 to *Ubx* TREs in third-leg imaginal discs. (**A**) PCR analysis of NChIP assays detecting the association of Ash1 with *bxd* DNA elements in mock- and RNase-treated chromatin isolated from third-leg imaginal discs. (**B**) RT-PCR analyses of NChIP immunoprecipitates detecting the association of Ash1 with TRE transcripts in native chromatin. (**C**) RT-PCR analyses of NChIP assays detecting the association of Ash1 with TRE transcripts in chromatin and the soluble, histone-free nuclear extract. (**D**) RT-PCR analysis of XChIP RNA immunoprecipitates detecting chromatin-associated *bxd* transcripts (top) and the corresponding *bxd* DNA templates (bottom) in chromatin isolated from wild-type (WT) and *ash1*^{22} mutant third-leg discs. Chromatin was immunoprecipitated with antibodies to dimethylated H3-K9 or rat serum (C). In all panels, input represents the amount of TREs and TRE transcripts detected in 0.5% of the starting material.

mock- and RNase-treated chromosome squashes. Compared to mock-treated chromosomes, RNase treatment attenuated the association of Ash1 with the majority of the target loci (fig. S9). This result suggests that RNA plays an important role in the recruitment of Ash1 to target genes in chromatin.

Ash1 associates with chromatin-bound TRE transcripts. To assess whether TRE transcripts associate with chromatin, we investigated whether Ash1 coprecipitates TRE transcripts from chromatin-free nuclear extract. Ash1 bound TRE transcripts in chromatin but not chromatin-free nuclear extract (Fig. 4C) (fig. S8), indicating that TRE transcripts are preferentially associated with chromatin in the cell.

We used XChIP to determine whether the association of Ash1 with TRE transcripts precedes the recruitment of Ash1 to TREs in chromatin, or vice versa. In vivo cross-linked chromatin was isolated from wild-type and *ash1*^{22} mutant third-leg discs, sheared, and immunoprecipitated with antibodies to dimethylated H3-K9 present at the TREs of the transcriptionally active and inactive *Ubx* locus in third-leg discs (Fig. 2, A and B). The antibody to dimethylated H3-K9 coprecipitated with TREs and TRE transcripts from the chromatin of wild-type and *ash1*^{22} third-leg discs (Fig. 4D) (fig. S10), indicating that TRE transcripts are retained at *Ubx* TREs before recruitment of Ash1.

TRE transcripts recruit Ash1 in trans. To dissect the role of TRE transcripts in *Ubx* transcription, we asked whether transiently transcribed TRE transcripts could restore the recruitment of Ash1 to *Ubx* TREs and *Ubx* expression in S2 cells, which express Ash1 but lack endogenous TRE transcripts. S2 cells were transiently transfected with plasmids transcribing sense or antisense TRE transcripts (*19*) (Fig. 5A) (fig. S11). In PCR assays, *Ubx* transcription was undetectable in S2 cells transiently transcribing antisense TRE transcripts or *mdu* (Fig. 5, A and B). In contrast, *Ubx* transcription was activated by one TRE transcript (Fig. 5B) (fig. S11) and cooperatively activated by multiple TRE transcripts (fig. S12).

We next used XChIP to determine whether activation of *Ubx* transcription by transient TRE transcripts coincides with the recruitment of Ash1 to TREs. In vivo cross-linked chromatin was isolated from wild-type S2 cells and cells transiently transcribing one or multiple TRE transcripts and control RNAs, and it was then immunoprecipitated with antibodies to Ash1 and the Ash1 histone methylation pattern (Fig. 5C). Ash1 was not detected at the TREs of transcriptionally silent *Ubx* in cells transcribing *mdu* or antisense TRE RNAs (Fig. 5C). In contrast, Ash1 and the Ash1 histone methylation pattern were detected at the *Ubx* TREs in cells transcribing TRE1(+), TRE2(+), and/or TRE3(+) (Fig. 5C) (fig. S13). Each of the three TRE transcripts facilitated the association of Ash1 only with the corresponding template TRE but not with other TREs.

To verify the specificity of the described recruitment, we investigated whether TRE transcripts facilitate recruitment of Ash1 to CMEs containing TREs/PREs and genes other than *Ubx*. In XChIP assays, Ash1 was not detected at *Drosophila* genes and the CMEs *MCP* and *Fab7* in S2 cells transcribing TRE1(+), TRE2(+), or TRE3(+) (fig. S14) (*12*, *13*). Thus, TRE transcripts facilitate Ash1 recruitment specifically to the corresponding TRE template DNA.

We used NChIP and XChIP to assess whether transiently transcribed TRE transcripts associate with TREs and Ash1 in chromatin. Native chromatin was isolated from wild-type S2 cells and S2 cells transiently cotranscribing all three sense or antisense TRE transcripts. Ash1 did not associate with TRE transcripts (Fig. 5, D and F) and TREs (Fig. 5, E and G) in cross-linked (Fig. 5, D and E) and native chromatin (Fig. 5, F and G) from S2 cells transcribing *mdu*. In contrast, Ash1 interacted with TREs and TRE transcripts in S2 cells cotranscribing TRE1(+), TRE2(+), and TRE3(+) (Fig. 5, D to G) (fig. S11).

The association of Ash1 with TREs and TRE transcripts was attenuated by RNase A and RNase H but not RNase III (Fig. 5, D to G) (fig. S11). RNase treatment did not abolish the association of TBP with the *Ubx* promoter (Fig. 5, E and G). These results indicate that Ash1 associates with TRE transcripts and TREs in vivo and that TRE transcripts mediate the association of Ash1 with TREs in trans.

To test this hypothesis, we used RNA interference (RNAi) to assess whether degradation of TRE transcripts attenuates recruitment of Ash1 to *Ubx* TREs and *Ubx* expression in third-leg discs (*27*). In vitro cultivated third-leg discs were incubated with small interfering RNAs (siRNAs) targeting all three TRE transcripts or with control siRNA. RT-PCR and XChIP assays indicated that siRNA-mediated degradation of TRE transcripts attenuates *Ubx* transcription and the interaction of Ash1 with TREs (Fig. 6, A and B) (fig. S15).

Next, we used the binary Gal4/UAS system to determine whether ectopic transcription of TRE transcripts restores recruitment of Ash1 to *Ubx* TREs and *Ubx* transcription (*28*). Effector flies carrying a heat-inducible driver (hsp70Gal4) were crossed with reporter flies carrying Gal4-dependent reporter genes (UAS-TRE) consisting of Gal4-responsive UAS DNA sites and a promoter driving the transcription of

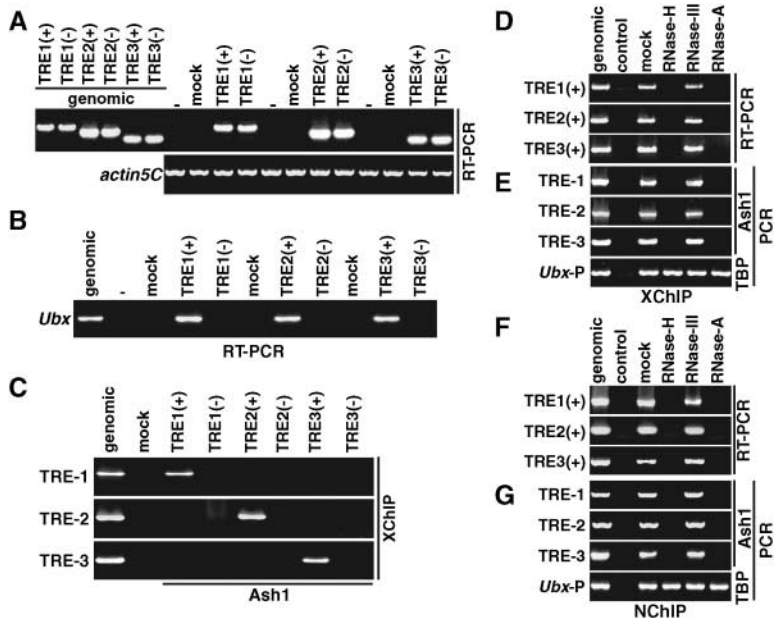

Fig. 5. TRE transcripts reconstitute the interaction of Ash1 with *Ubx* TREs and *Ubx* transcription in S2 cells. (**A**) PCR analysis detecting TRE transcripts and *actin5C* transcription in wild-type S2 cells (–) and S2 cells transfected with plasmids transcribing *mdu* (mock), TRE transcripts [TRE1(+), TRE2(+), TRE3(+)], or antisense TRE transcripts [TRE1(–), TRE2(–), TRE3(–)]. (**B**) PCR assays as in (A) but detecting *Ubx* transcription in wild-type and transfected S2 cells. (**C**) PCR analysis of immunoprecipitates detecting the association of Ash1 with *Ubx* TREs in S2 cells transcribing *mdu* (mock) or sense and antisense TRE transcripts. (**D** and **E**) RT-PCR and PCR analyses of immunoprecipitates detecting the association of Ash1 with *Ubx* TRE transcripts (D) and TREs (E) and TBP with the *Ubx* promoter (*Ubx*-P) (E) in chromatin from S2 cells transiently cotranscribing TRE1(+), TRE2(+), and TRE3(+). (**F** and **G**) RT-PCR (F) and XChIP assays (G) as in (D) and (E), except that native chromatin was used. Transcripts and DNA elements detected in *Drosophila* genomic DNA are also shown.

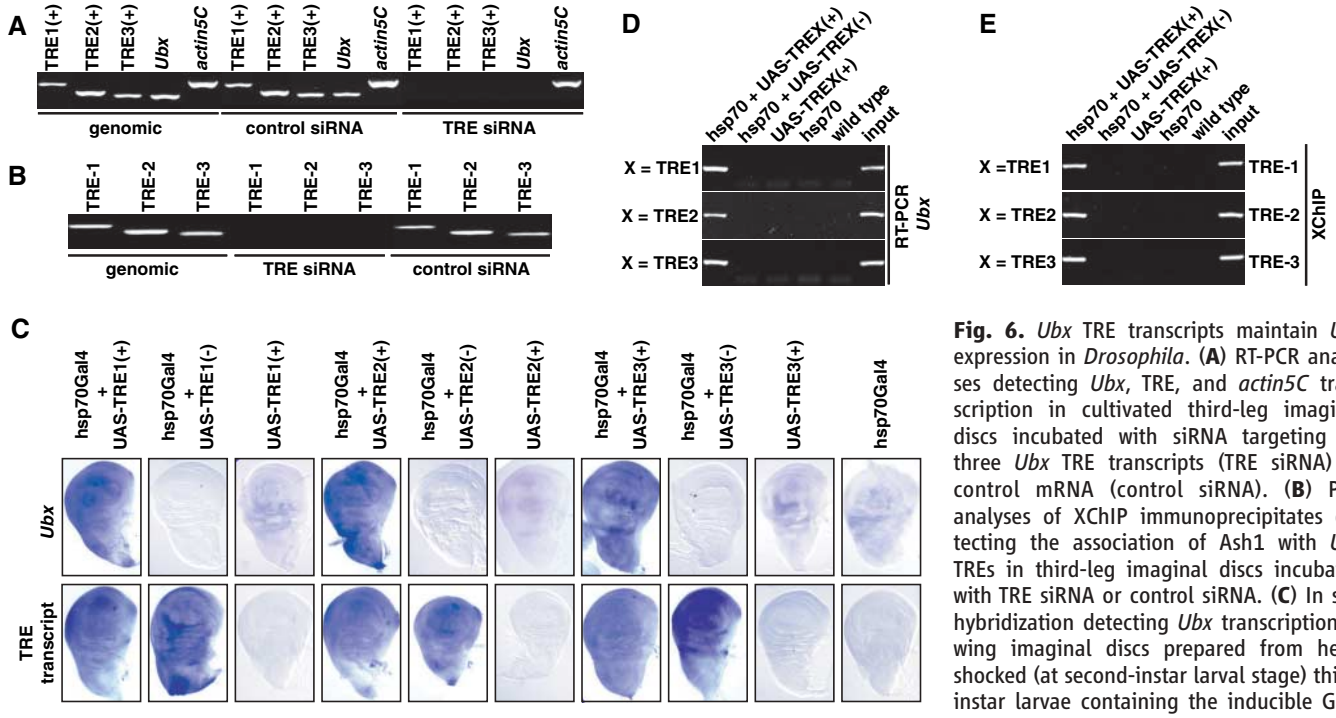

Fig. 6. *Ubx* TRE transcripts maintain *Ubx* expression in *Drosophila*. (**A**) RT-PCR analyses detecting *Ubx*, TRE, and *actin5C* transcription in cultivated third-leg imaginal discs incubated with siRNA targeting all three *Ubx* TRE transcripts (TRE siRNA) or control mRNA (control siRNA). (**B**) PCR analyses of XChIP immunoprecipitates detecting the association of Ash1 with *Ubx* TREs in third-leg imaginal discs incubated with TRE siRNA or control siRNA. (**C**) In situ hybridization detecting *Ubx* transcription in wing imaginal discs prepared from heat-shocked (at second-instar larval stage) third-instar larvae containing the inducible Gal4 driver (hsp70Gal4) and/or Gal4-dependent reporter plasmids (UAS-TRE) transcribing sense (+) or antisense (–) *Ubx* TRE transcripts. (**D**) RT-PCR analyses detecting *Ubx* transcription in wing imaginal discs described in (C). (**E**) PCR analyses of XChIP immunoprecipitates detecting the association of Ash1 with *Ubx* TREs in wing imaginal discs described in (C).

sense and antisense TRE transcripts. Heat treatment of second-instar larvae resulted in ectopic transcription of TRE transcripts in all imaginal discs of third-instar larvae. Ectopic transcription of each TRE transcript nucleated ectopic transcription of *Ubx* in wing imaginal discs (Fig. 6, C and D) (figs. S15 and S16) and facilitated the recruitment of Ash1 to the corresponding *Ubx* TREs (Fig. 6E). It is noteworthy that ectopic TRE transcription in second-instar larvae caused lethality in pupae. In contrast, ectopic *Ubx* expression was not observed in discs prepared from heat-treated parental strains and discs transcribing antisense TRE transcripts (Fig. 6C).

Transcription of antisense TRE transcripts attenuated endogenous transcription of *Ubx* in wing discs isolated from young third-instar larvae, which suggests that ectopic transcription of antisense RNA interferes with the TRE transcript–mediated recruitment of Ash1 to *Ubx* TREs. In summary, our data provide evidence that noncoding TRE transcripts facilitate activation of *Ubx* expression by recruiting Ash1 to the *Ubx* TREs in the fly.

Discussion. Noncoding RNAs play an important role in the recruitment of proteins in several epigenetic phenomena. Recent studies have linked siRNAs to heterochromatin formation and transcriptional silencing of transgenes and transposons (*29*, *30*). SiRNAs facilitate the recruitment of HMTs and DNA methyltransferases to chromatin (*31*, *32*). In *Schizosaccharomyces pombe*, heterochromatic silencing involves the RNA-induced initiator of transcriptional gene silencing complex (RITS), which contains an siRNA component that is essential for the recruitment of RITS to heterochromatic loci (*31*). The inability of RNase III, the key enzyme of the RNAi machinery, to degrade TRE transcripts into siRNAs and the interaction of Ash1 with full-length TRE transcripts in chromatin strongly argues against the involvement of siRNAs in the described RNA-dependent recruitment of Ash1 to chromatin.

Long ncRNAs are key players in imprinting and gene dosage compensation (*22*, *27*, *33*). In *Drosophila*, gene dosage compensation is achieved by a global twofold up-regulation of transcription from the male X chromosome and depends on the activity of the dosage compensation complex (DCC) that contains male-specific proteins and two ncRNAs, *RNA on X 1* (*rox1*) and *RNA on X 2* (*rox2*) (*20*). Both RNAs are transcribed by single-copy genes that, as well as several other X chromosome regions, serve as chromatin entry sites for the DCC on paternal X chromosomes (*20*, *27*). *Rox1* and *Rox2* facilitate the assembly and recruitment of the DCC to chromatin entry sites (*20*). In mammals, spreading of *Xist* RNA culminates in X chromosome inactivation (*22*). Current models propose that the association between ncRNAs and chromatin involves their interaction with proteins, nascent transcripts at template DNA, or the template DNA (*27*, *34*). The observed attenuation of the association between TRE transcripts and TREs by RNase H suggests that TRE transcripts are retained at TREs through hybridization with the corresponding template DNA. Because none of the known DNA repair systems targets DNA-RNA hybrids, RNA-DNA hybrids represent stable molecular entities that, in general, may anchor ncRNAs at corresponding DNA templates in chromatin (*35*).

The three TRE transcripts of *Ubx* do not share common sequence motifs. This is not surprising, because the functionally redundant *rox* RNAs and functionally identical regions in *Xist*, which are required for chromatin localization and protein recruitment, lack identifiable sequence motifs (*27*). Because many RNA-protein interactions are facilitated by RNA secondary structures, the interaction of Ash1 with TRE transcripts might be mediated by secondary RNA structures rather than sequence motifs. In addition, the specificity of RNA-protein interactions is often generated by induced-fit mechanisms that involve complex, extensive conformational changes in both proteins and the target RNA generating a specific interaction surface (*36*, *37*).

Rox1 and *rox2* RNAs transcribed from autosomes can localize to and mediate gene dosage compensation on the male X chromosome, indicating that the chromatin entry of *rox* RNAs does not depend on transcription of chromatin entry sites in cis (*38*). Thus, the association of transiently transcribed TRE transcripts with TREs in S2 cells suggests that TREs function as chromatin entry sites for the corresponding TRE transcripts in trans and cis, and that the transcription and

chromatin entry site activities of TREs are functionally separated. Cumulatively, our results support a model in which RNAs transcribed from the TREs of *Ubx* are retained at TREs through DNA-RNA interactions and provide a RNA scaffold that is bound by Ash1.

References and Notes

1. R. Jaenisch, A. Bird, *Nat. Genet.* **33** (suppl.), 245 (2003).
2. B. M. Turner, *Cell* **111**, 285 (2002).
3. V. Orlando, *Cell* **112**, 599 (2003).
4. L. Ringrose, R. Paro, *Annu. Rev. Genet.* **38**, 413 (2004).
5. A. Breiling, V. Orlando, *Nat. Struct. Biol.* **9**, 894 (2002).
6. P. B. Becker, W. Horz, *Annu. Rev. Biochem.* **71**, 247 (2002).
7. T. Jenuwein, C. D. Allis, *Science* **293**, 1074 (2001).
8. R. Cao, Y. Zhang, *Curr. Opin. Genet. Dev.* **2**, 155 (2004).
9. C. Beisel, A. Imhof, J. Greene, E. Kremmer, F. Sauer, *Nature* **419**, 857 (2002).
10. N. Tripoulas, D. LaJeunesse, J. Gildea, A. Shearn, *Genetics* **143**, 913 (1996).
11. D. LaJeunesse, A. Shearn, *Mech. Dev.* **53**, 123 (1995).
12. S. Schmitt, M. Prestel, R. Paro, *Genes Dev.* **19**, 697 (2005).
13. G. Rank, M. Prestel, R. Paro, *Mol. Cell. Biol.* **22**, 8026 (2002).
14. E. Bae, V. C. Calhoun, M. Levine, E. B. Lewis, R. A. Drewell, *Proc. Natl. Acad. Sci. U S A.* **99**, 16847 (2002).
15. H. D. Lipshitz, D. A. Peattie, D. S. Hogness, *Genes Dev.* **1**, 307 (1987).
16. J. Dejardin *et al.*, *Nature* **434**, 533 (2005).
17. T. Rozovskaia *et al.*, *Mol. Cell. Biol.* **19**, 6441 (1999).
18. C. H. Martin *et al.*, *Proc. Natl. Acad. Sci. USA* **92**, 8398 (1995).
19. See supporting material on *Science* Online.
20. A. Akhtar, *Curr. Opin. Genet. Dev.* **13**, 161 (2003).
21. A. Wutz, *Bioessays* **25**, 434 (2003).
22. E. Heard, *Curr. Opin. Cell Biol.* **16**, 247 (2004).
23. M. A. Matzke, J. A. Birchler, *Nat. Rev. Genet.* **6**, 24 (2005).
24. W. A. Krajewski, T. Nakamura, A. Mazo, E. Canaani, *Mol. Cell. Biol.* **25**, 1891 (2005).
25. S. R. Albright, R. Tjian, *Gene* **242**, 1 (2000).
26. T. Maile, S. Kwoczynski, R. J. Katzenberger, D. A. Wassarman, F. Sauer, *Science* **304**, 1010 (2004).
27. H. Kawasaki, K. Taira, *Curr. Opin. Mol. Ther.* **7**, 125 (2005).
28. C. B. Phelps, A. H. Brand, *Methods* **14**, 367 (1998).
29. E. J. Sontheimer, *Nat. Rev. Mol. Cell Biol.* **6**, 127 (2005).
30. V. Schranke, R. Allshire, *Curr. Opin. Gen. Gev.* **14**, 174 (2004).
31. A. Verdel *et al.*, *Science* **303**, 672 (2004); published online 2 January 2004 (10.1126/science.1093686).
32. M. J. O'Neill, *Hum. Mol. Genet.* **14** Spec No 1:R113 (2004).
33. S. W.-L. Chan *et al.*, *Science* **303**, 1336 (2004).
34. S. I. Grewal, J. C. Rice, *Curr. Opin. Cell Biol.* **16**, 230 (2004).
35. M. Christmann, M. T. Tomicic, W. P. Roos, B. Kaina, *Toxicology* **193**, 3 (2003).
36. Y. Chen, G. Varani, *FEBS J.* **272**, 2088 (2005).
37. F. H. Allain, P. W. Howe, D. Neuhaus, G. Varani, *EMBO J.* **16**, 5764 (1997).
38. V. H. Meller, B. P. Rattner, *EMBO J.* **21**, 1084 (2002).

39. We thank J. A. Diaz-Pendon, E. Poon, and M. Rubalcava for support with RACE, tissue culture, and disc preparation, and members of the Sauer lab for helpful comments that improved the manuscript. F.S. thanks S. Angle for support. Supported by Deutsche Forschungsgemeinschaft (DFG) research fellowship SA1010/1-1 (T.S.-E.), a DFG/Transregio-5 grant (E.K.), and NIH grant GM073776 and VolkswagenStiftung grant I/79-725 (F.S.).

Supporting Online Material

www.sciencemag.org/cgi/content/full/311/5764/1118/DC1
Materials and Methods
Figs. S1 to S16
Tables S1 to S3
References

20 July 2005; accepted 23 January 2006
10.1126/science.1117705

A Swimming Mammaliaform from the Middle Jurassic and Ecomorphological Diversification of Early Mammals

Qiang Ji,[1,3] Zhe-Xi Luo,[2,1]* Chong-Xi Yuan,[3] Alan R. Tabrum[2]

A docodontan mammaliaform from the Middle Jurassic of China possesses swimming and burrowing skeletal adaptations and some dental features for aquatic feeding. It is the most primitive taxon in the mammalian lineage known to have fur and has a broad, flattened, partly scaly tail analogous to that of modern beavers. We infer that docodontans were semiaquatic, convergent to the modern platypus and many Cenozoic placentals. This fossil demonstrates that some mammaliaforms, or proximal relatives to modern mammals, developed diverse locomotory and feeding adaptations and were ecomorphologically different from the majority of generalized small terrestrial Mesozoic mammalian insectivores.

The Middle Jurassic mammalian diversification gave rise to several emergent clades: basal eutriconodontans, amphitheriid cladotherians, the basal mammalian lineage of shuotheriids, and basal australosphenidans (*1*–*5*). These new clades of crown Mammalia coexisted with several mammaliaform lineages (the proximal relatives to modern mammals) (*1*, *6*–*8*). Docodontans are a Mesozoic mammaliaform lineage that have specialized molars for omnivorous feeding; several taxa are known from the Middle Jurassic (*1*, *9*–*13*). Here, we report on a large docodontan mammaliaform that has some dental features for feeding on aquatic invertebrates and small vertebrates, plus specialized skeletal and soft-tissue features for swimming and burrowing.

Description and comparison. *Castorocauda lutrasimilis*, gen. et sp. nov. (*14*), is from the Middle Jurassic Jiulongshan Formation, dated to be approximately 164 million years ago (*15*–*17*). The fauna includes pterosaurs (*17*, *18*), a coelurosaurian dinosaur (*19*), lissamphibians (*20*), abundant fossil insects (*21*), and the conchostracan *Euestheria* (*22*). The holotype of *C. lutrasimilis* (Fig. 1) is represented by a partial skeleton (preserved rostrum-tail length ≥425 mm) with incomplete cranium (preserved length ≥60 mm) but well-preserved mandibles and lower dentition (incisors 4, canine 1, premolars 5, molars 6). Lower molars 3 to 6 have the diagnostic characteristics of docodontans (Fig. 2): anteriorly placed and enlarged lingual cusp g, triangulated crests formed by cusps a-c and a-g, and two partially enclosed basins formed respectively by cusps a, b, and g, and by cusps a, c, and d (*9*–*12*). As in all docodontans, the molars were capable of both shearing by the triangulated crests and grinding between the anterior (''pseudotalonid'') basin and the transversely widened upper molars (*9*–*12*). *Castorocauda* is distinctive from other docodontans in having mediolaterally compressed crowns of molars 1 and 2, each with five cusps in straight alignment (*23*, *24*); primary cusp a and posterior cusps c and d are slightly recurved (Fig. 2). These ''triconodont-like'' anterior molars are plesiomorphic for mammaliaforms (*6*–*8*) but nonetheless distinctive among docodontans. They are convergent to those of placental mesonychians and Eocene whales (*25*). This type of molar with recurved cusps in alignment is hypothesized to be a specialization for feeding on fish and aquatic invertebrates by functional analogy to the teeth of modern pinniped carnivores such as seals.

Castorocauda is preserved with intact middle ear bones (Fig. 2) on the mandible, including the articular (malleus), the surangular, and the angular (ectotympanic). The middle ear bones in anatomical association with the mandible corroborate a previous interpretation of the middle ear in docodontans (*26*). A concavity on the

[1]Department of Earth Science, Nanjing University, Nanjing 200017, China. [2]Carnegie Museum of Natural History, Pittsburgh, PA 15213, USA. [3]Chinese Academy of Geological Sciences, Beijing 100037, China.

*To whom correspondence should be addressed. E-mail: LuoZ@CarnegieMNH.org